Rigo, Davide; Fechter, Tijana; Capanema, Ewellyn; Diment, Daryna; Alopaeus, Marie; Tarasov, Dmitry; Cantero, Danilo; Balakshin, Mikhail

Isolation of β-O-4-Rich Lignin From Birch in High Yields Enabled by Continuous-Flow Supercritical Water Treatment

Published in:
ChemSusChem

DOI:
10.1002/cssc.202401683

Published: 02/01/2025

Document Version
Publisher's PDF, also known as Version of record

ChemSusChem

Research Article
doi.org/10.1002/cssc.202401683

Chemistry Europe
European Chemical Societies Publishing

www.chemsuschem.org

Isolation of β-O-4-Rich Lignin From Birch in High Yields Enabled by Continuous-Flow Supercritical Water Treatment

Davide Rigo,*[a] Tijana Fechter,[b] Ewellyn Capanema,*[c] Daryna Diment,[a] Marie Alopaeus,[d] Dmitry Tarasov,[a] Danilo Cantero,[b] and Mikhail Balakshin+[a]

The continuous flow supercritical water (scH_2O) treatment of Birch wood (T = 372–382 °C; t = 0.3–0.7 s; p = 260 bar) followed by alkali extraction of lignin allowed for the isolation of lignin and lignin carbohydrate complexes (LCCs) with a high number of β-O-4 moieties in the range 29–57/100 Ar (evaluated by quantitative ^{13}C NMR analysis) in yields ranging between 13–19 wt% with respect to the initial wood. A "lightning rod effect" of carbohydrates has been claimed to explain the low degradation of β-O-4 bonds during the process. The structure of the isolated lignin was thoroughly elucidated via comprehensive NMR studies (HSQC, ^{13}C and ^{31}P). A low degree of condensation (DC) < 5% was found for all the lignin samples, which was only slightly dependent on the reaction severity. The number of aliphatic −OH, phenolic −OH, and −COOH groups was in the range 3.37–5.25, 1.41–2.31 and 0.39–0.73 mmol/g, respectively. The number of −COOH groups increased with increased severity, suggesting that oxidation can occur during the scH_2O treatment. Furthermore, by simply varying the reaction severity, it was possible to tune important lignin properties, like the molar mass and the glass transition temperature (T_g).

Introduction

One of the main challenges to achieve lignocellulosic biomass fractionization is its recalcitrance.[1–3] The nature and the interaction between the major biomass components (lignin, cellulose and hemicellulose) create a stress resistant structure in plants cell wall, which requests efforts to be broken down.[4] Various methods are reported in the literature for biomass fractionation, like acid[5,6] and alkali treatments,[2] and enzymatic hydrolysis.[7] Such strategies pose some drawbacks. Enzymatic hydrolysis requests pre-treatment steps to facilitate the enzymatic digestibility and to be more effective.[8] These additional sequential steps make the overall procedure more costly compared to one-step processes. Acid treatment of wood generally requests high acid concentration (over 30%) at moderate temperatures (T < 100 °C).[9] In that regard, the high corrosivity of inorganic acids (*i.e.*, sulfuric acid) not only represents an engineering challenge in the reactor design but also might cause health hazard to the Lab operators. Though alkali-mediated fractionation is one of the most used and effective method, it promotes several side and unwanted reactions in lignin such as the cleavage of β−O–aryl units.[2] Other strategies are based on hot water treatments.[10–13] Nevertheless, they generally require long reaction times (t > 1 h) and high temperature (130 °C < T < 250 °C) to achieve separation of the carbohydrate fractions from lignin.

An alternative method for biomass fractionation is via supercritical water (scH_2O) treatment.[14–17] Such an approach is attractive because the biomass separation can be achieved within short time (t < 1 min)[18] and since water is an inexpensive and non-toxic reaction medium. Intriguingly, water at the supercritical state (T_c = 374 °C, p_c = 22.1 MPa) dramatically changes its characteristics when compared to its behavior at ambient conditions. To summarize: i) the dielectric constant of scH_2O decreases, leading to an increased affinity towards organic compounds; ii) the number of H-bonds decreases; iii) the ionic product of water (K_w) decreases from 10^{-14} at room temperature and pressure to 10^{-22} at 400 °C and 25 MPa,[19] becoming highly neutral medium. In addition, the scH_2O properties can be easily tuned by adjusting the reactions parameters (mainly pressure and temperature).[19]

Numerous studies reported the use of scH_2O as reaction medium for the treatment[20,21] and gasification[22–26] of wood, and reforming of lignin oil.[27] Such topics have been thoroughly reviewed elsewhere.[28–30] The scH_2O fractionation of Birch wood received little attention in batch. For instance, Quian et al. investigated the $NaCO_3$-catalyzed liquefaction of birch wood with sub- and supercritical water to yield bio-oils.[31] Azadi et al.

[a] *Department of Bioproducts and Biosystems, Aalto University, Espoo, Finland*
[b] *The Institute of Bioeconomy. Calle Dr Mergelina S/N, Department of Chemical Engineering and Environmental Technology, University of Valladolid, Valladolid, Spain*
[c] *RISE Research Institutes of Sweden Division Bioeconomy, Stockholm*
[d] *Laboratory of Natural Materials Technology, Åbo Akademi University, Turku, Finland*

Correspondence: *Davide Rigo, Department of Bioproducts and Biosystems, Aalto University, Vuorimiehentie 1, Espoo 02150 E-mail, Finland.*
Email: davide.rigo@unive.it

Ewellyn Capanema, RISE Research Institutes of Sweden Division Bioeconomy, Box 5604, 114 86 Stockholm.
Email: ewellyn.capanema@ri.se

[+] *Deceased, 2022.*

Supporting Information for this article is available on the WWW under https://doi.org/10.1002/cssc.202401683

studied the production of H_2 from birch wood bark.[32] However, to the best of our knowledge no reports refer to the use of continuous flow scH_2O systems for the fractionation of Birch wood.

Continuous flow represents a valuable opportunity to carry out biomass fractionation using supercritical water as the reaction medium. Hence, IUPAC ranked continuous flow (CF) technologies among the "Top Ten Emerging Technologies in Chemistry",[33] due to their several outstanding features, like an improved heat transfer, a decrease in the equipment size/production capacity ratio, and minor energy consumption and waste generation, among others.[34] An almost instantaneous mixing is usually achieved in micro-structured reactors, which allows to decrease the reaction time and energy consumption (process intensification).[35] In addition, CF enables for a quick variation of reaction conditions (T, *p*, flow rate, concentration, etc.), leading to rapid reaction optimization.

Our group exploited the advantages of CF chemistry and scH_2O for the implementation of a scH_2O CF system for biomass fractionation. This system was created by the University of Valladolid in 2009.[36] The main advantages are: extremely fast heating of biomass (from room temperature to more than 375 °C); precise control of reaction time by reactor volume and flows, and extremely fast cooling by applying the Joule-Thompson effect. With such apparatus, we have been able to recover cellulose and hemicellulose fractions from biomass,[15] to convert sugars-rich biomass into lactic acid,[16] for cellulose hydrolysis,[17,37] for the upgrading of glucose,[38] and for refining lignin-rich agro-waste.[14]

One last aspect to be highlighted is that a high number of β-O-4 bonds is desired in the isolated lignins. For instance, it facilitates lignin depolymerization and leads to an increased yield of monomers/dimers *via* reductive/oxidative protocols.[39] In addition, we recently found a positive correlation between the number of β-O-4 units and the lignin sorption capacity.[40] Various methods are reported to protect the "native lignin" structure, such as aldehydes-mediated processes,[41,42] flow through systems,[43] oxidations,[44] and cyclic extraction.[45] However, to the best of our knowledge the use of scH_2O has not been accounted as a method to minimize the cleavage of β-O-4 bonds during biomass fractionation.

The combination of our expertise in continuous flow scH_2O processes and in the NMR characterization of biorefinery lignins[12,13,46] prompted us to implement a scH_2O-mediated process for the fractionation of Birch wood and the subsequent lignin isolation and characterization. In this work, the fractionation of hardwood (Birch wood) using continuous flow scH_2O as the reaction medium was studied. The main purpose of this study was to investigate the impact of the scH_2O reaction conditions on the structure and properties of the isolated lignins. A comprehensive characterization of the isolated lignins was performed by 2D HSQC, ^{13}C and ^{31}P NMR analyses, DSC and GPC.

Experimental

Materials

Sodium hydroxide (NaOH), sulfuric acid (H_2SO_4), chromium (III) acetylacetonate, ($Cr(acac)_3$), endo-n-hydroxy-5-norbornene-2,3-dicarboximide (e-HNDI), 2-chloro-4,4,5,5-tetramethyl-1,3,2-dioxaphospholane (TMDP), deuterated dimethyl sulfoxide (DMSO-d_6), deuterated chloroform ($CDCl_3$), P_2O_5, and pyridine (all analytical grades) were purchased from Sigma-Aldrich.

Continuous Flow scH_2O Treatment of Birch Wood

Biomass pre-treatment. Silver Birch (*Betula Pendula*) wood chips were firstly ground into sawdust (average particle size 2 mm) using a knife mill. Then, in order to provide proper pumping of the biomass through the continuous flow reactor, the sawdust was further milled using ball milling (Retsch) for 2 hours at room temperature using 14 minutes of break after 1 minute of milling.

Supercritical water hydrolysis pilot plant. A detailed description of the CF setup can be found in a previous work.[14] Briefly, the setup allows a precise control of the reaction time and temperature. Temperature is designed by enthalpy balance of the 2 mixed streams at the inlet of the reactor (milled wood slurry and scH_2O). Then the designed conditions are used as targets for the experiments. The control of the reaction time was performed by adjusting the reactor volume and the flow. The homogeneity of wood and scH_2O in the mixer allows fast heating and prevent potential degradation reactions during the heat-up ramps. The reactor geometry and high Reynolds number ensure good mixing. After the treatment, the temperature of the reactor was dropped down to 150 °C by applying the Joule-Thomson effect. Due to this fast cooling all reactions are mostly "frozen". The reactor operates with fluctuations of temperature and pressure of ± 2 °C and ± 5 bar, respectively.

Supercritical water treatment of Birch wood. The scH_2O treatment was carried out by continuously delivering a milled wood (Birch) aqueous slurry (liquid-to-solid ratio = 5 wt%) into a Sudden Expansion Reactor (SER).[16] The experiments were carried out at a 10 Kg/h scale (Kg are referred to the slurry), meaning 0.5 Kg/h of treated biomass. The reaction was carried out at T = 372–382 °C, p = 250 bar, and t = 0.3–0.7 s. At the end of the reaction, the two obtained soluble and insoluble fractions were separated by centrifugation at 4000 rpm for 20 minutes.

Lignin Isolation From the Treated Slurry

The wet solid residue obtained after the scH_2O treatment were freeze dried using Labconco Freezone 2.5. Then, about 2 g of freeze-dried sample was alkali extracted (NaOH aq. 1 wt%; 4x20 mL aliquots). The extracted lignin was then precipitated to pH = 2.5 by adding a diluted H2SO4 mixture (C = 0.5 M), followed by filtration on a glass crucible (pore size 5–15 μm). The filtered lignin samples were exhaustively washed with

deionized water (100 mL) and then dried on a vacuum oven (T = 40 °C, $p = 5$ mbar) using P_2O_5 as dehydrating agent until constant weight. The yield was evaluated gravimetrically, and the samples were analyzed by NMR (HSQC, ^{13}C and ^{31}P), DSC and SEC. The lignin samples were labelled S1–4 based on increased severity (Table S1).

Nuclear Magnetic Resonance (NMR) Spectroscopy

General. The HSQC spectra were recorded with a Bruker AVANCE 600 NMR spectrometer equipped with a CryoProbe. ^{31}P and ^{13}C NMR analysis were performed with a Bruker AV III 400 MHz spectrometer. The HSQC and ^{31}P NMR spectra are reported in the ESI, while the ^{13}C spectra are present in the main text. Reliable quantitative data about β-O-4 bonds and other moieties in lignin samples are obtained using a combination of different nuclear magnetic resonance (NMR) spectroscopy techniques, such as 2D experiments, quantitative ^{13}C, and ^{31}P.[47,48]

2D HSQC. The experimental procedure was carried out as we recently reported.[12] Briefly, 80 mg of sample was dissolved in 0.6 mL DMSO-d_6. The acquisition time was set at 77.8 ms for the ^{1}H-dimension and 36 scans per block were collected using the 1024 collected complex points. For the ^{13}C-dimension the acquisition time was 3.94 ms and 256-time increments were recorded. The 2D HSQC NMR data were manipulated with 1024x1024 data points applying the Qsine function for both ^{1}H and ^{13}C dimensions. The DMSO peak at δ_C/δ_H 39.5/2.49 ppm/ppm was used for calibration of the chemical shifts. The cross-peaks were assigned based on the previous reports.[12,13,49] The quantity of different lignin and LCC signals was normalized using an assumption of:

$$G + S = G_2 + S_{2,6}/2 = 100Ar \quad (1)$$

This assumption implies that the condensation at the positions of G_2 and $S_{2,6}$ of lignin is insignificant. All lignin samples were analyzed based on this procedure.

^{31}P NMR. The amounts of different hydroxyl groups were determined by ^{31}P NMR spectroscopy according to our optimized protocol.[50] The acquisition time and the relaxation delay were 1 s and 5 s, correspondingly; 128 scans were collected. Dry lignin samples (40.00 mg) were dissolved completely in a 1.6/1 (v/v) pyridine/$CDCl_3$ solution (0.4 mL) in a 5 mL vial. To this mixture, an internal standard (IS) solution (100 μL) of endo-N-hydroxyl-5-norbornene-2,3-dicaroboximide (e-HNDI) in 1.6/1 (v/v) pyridine/$CDCl_3$ (C = 20 mg/mL) was added (IS:lignin = 0.3 μmol/mg) together with 50 μL of a relaxation agent (Cr-(acac)$_3$) solution in 1.6/1 (v/v) pyridine/$CDCl_3$ (C = 11.4 mg/mL). Then, 100 μL of phosphitylation reagent (2–chloro–4,4,5,5–tetramethyl–1,3,2-dioxaphospholane) was added to the mixture, which was stirred vigorously. The obtained solution was transferred into an NMR tube and ^{31}P NMR experiment was performed. This procedure has been applied for samples S2–4. The analysis of sample S1 was not possible due to its poor solubility both in the conventional pyridine/$CDCl_3$ system and in a modified ionic liquid-based solvent system.[51]

Quantitative ^{13}C. About 200 mg of dry sample was dissolved in 0.55 mL of DMSO-d_6 containing a relaxation reagent, chromium(III) acetylacetonate (6 mg/mL). Once the sample was fully dissolved, the viscous solution was carefully transferred to an NMR tube. The spectra were collected with a Bruker 400 MHz and inverse gate detection and a 90-pulse width were used for the quantitative ^{13}C NMR acquisition. The acquisition time was set to 1.2 s, the relaxation delay to 2 s, and the number of scans to 20000. The spectra were processed as described earlier.[52]

Properties of the Extracted Lignins

Differential scanning calorimetry (DSC). The glass transition temperature (T_g) was determined by differential scanning calorimetry (DSC) recorded on a Discovery DSC 250 by TA instruments. Both conventional DSC and modulated DSC (mDSC) was recorded for the determination. For conventional DSC 1–3 mg of sample was weighed into a TZero™ aluminum pan and was measured against an empty TZero™ as a reference. The samples were heated from 40 °C to 115 °C at 5 °C/min under a flow of nitrogen (50 mL/min). The temperature was kept at 115 °C for 2 min whereafter the temperature was decreased to −90 °C at 20 °C/min. Thereafter, the temperature was increased to 115–200 °C depending on the onset temperature for thermal degradation for each sample (Figure 6). The T_g was determined from the last heating ramp in the TRIOS v5.1.1.5 software.

For MDSC 4–12 mg sample was measured by first heating from 40 °C to 115 °C at 5 °C/min followed by cooling 20 °C (S4 was cooled to −50 °C). Thereafter the temperature was increased to 115–120 °C depending on the samples' onset temperature for thermal degradation. The modulation temperature was set to 1.20 °C and the modulation amplitude was 60 s. The T_g was determined from the last heating ramp in the reversible heat flow curve. The DSC curves for Samples S1 and S2 are reported in the ESI. For samples S3 and S4 it was not possible to clearly detected the T_g from the DSC curves. For this reason, they have not been reported in this work.

Molar mass distribution. The HPLC system used was Agilent 1100. The calibration curve was accomplished with polystyrene sulfonate standards (1000–64000 g/mol), ascorbic acid (176 g/mol) and NaCl (58 g/mol; detection with refractive index detector). Molar masses were determined based on the UV signal at 280 nm and the columns used were Polymer Standards Service MCX 300x8 mm (three columns with pore sizes of 100 Å, 500 Å, 1000 Å). Flow rate was 0.7 mL/min and injection volume 50 μL. Samples were dissolved in eluent (0.1 M NaOH) at the concentration of 2 mg/mL. The chromatograms are reported in the ESI section.

Results and Discussion

The scH_2O treatment of birch wood under continuous flow The isolation of the lignin samples was carried out following a multi-step procedure comprising i) a continuous flow scH_2O treatment of Birch wood followed by ii) alkali extraction of the obtained insoluble fraction (Figure 1). A severity factor was calculated to facilitate the analysis of the results. The severity factor is calculated via an equation that allows converting any pair of reaction temperature and time into a reaction time at a reference temperature.[37] In this way, it can be assumed that all the experiment were run at the same temperature and the treatment severity is a function of the reaction time calculated. Further details about this equation can be found in the previous paper.[37] The equation used for the calculations is:

$$t_s = t_T{}^{*} e^{\left[E_a \frac{T - T_{ref}}{T \cdot T_{ref} \cdot R}\right]} \quad (2)$$

Where "t_s" is the time adjusted by severity equation; "t_T" is the actual reaction time; "E_a" is the activation energy of the main reaction (in this case was cellulose hydrolysis); "T" is the actual reaction temperature; "T_{ref}" is the reference temperature (375 °C); and "R" is the universal gas constant. The activation energy for this calculation was 430 kJ/mol, as previously determined experimentally.[16]

The scH_2O treatment was carried out at a 0.5 Kg/h of treated biomass using a Supercritical water hydrolysis pilot plant (see experimental for more details). Scaling up to a continuous flow supercritical device offers several advantages. Firstly, the rapid reaction rates achievable under supercritical conditions allow for a reduction in reactor size requirements, enhancing efficiency and lowering costs. Secondly, the use of a continuous reactor, such as a Supercritical Extraction Reactor (SER), provides precise control over reaction times. The ability to cool down the reaction within less than 0.1 seconds prevents the formation of undesired materials by inhibiting lignin polycondensation reactions. This precise control not only improves the quality of the extracted lignin but also enhances the overall efficiency of the process. The main disadvantage of this process is the high energy demand of supercritical water, which can be reduced significantly by efficient energy integration.

Figure 2 shows the yields of products after scH_2O hydrolysis together with the alkali extracted lignin yield at the different reaction severities. As expected, the ratio of solids liquefaction is increased by increasing the reaction severity (time or temperature, or both). The yield of solids follows the opposite trend as it is correlated. The degree of liquefaction ranges between 24% and 76% under the tested reaction conditions. As expected, the

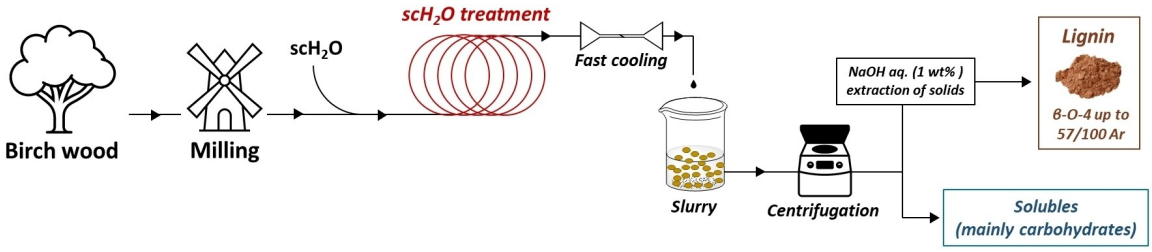

Figure 1. Overall procedure for the scH_2O treatment and subsequent isolation of lignin.

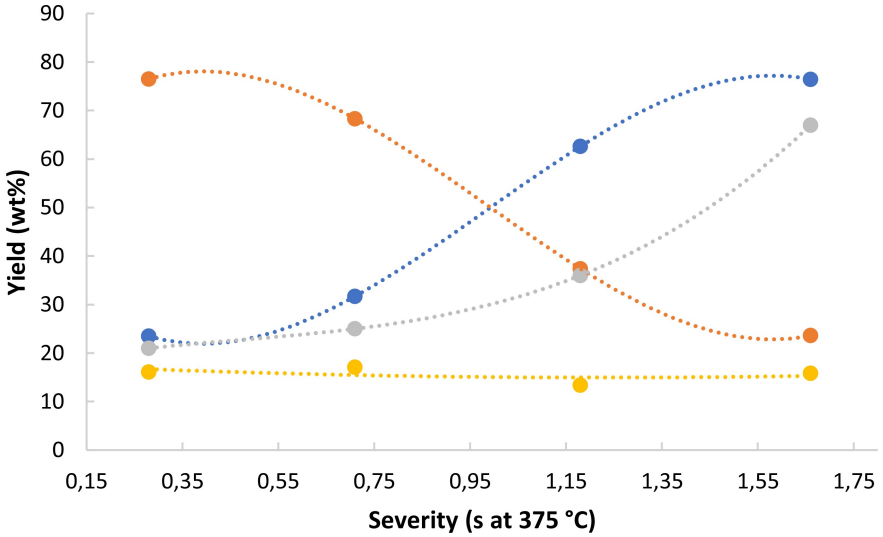

Figure 2. Products distribution at different severities. -•- Soluble fraction; -•- Insoluble fraction; -•- Lignin yield with respect to the insoluble fraction; -•- Lignin yield with respect to the initial wood.

lignin percentage in the insoluble fraction shows an increasing trend with both higher severity and liquefaction. This is consistent with the hydrolysis of the polysaccharide chains into monomeric sugars at high severity.

Regardless the treatment conditions, the amount of lignin recovered from biomass was around 15 wt% with respect to the initial wood. This suggests that even at the highest tested severity the scH_2O treatment preferably targets the hydrolysis of sugars. This is in line with our recent results on the ultrafast hydrolysis of polysaccharides for the production of monomeric sugars.[37] We here also propose the term "lightning rod effect" of sugars which will be further discussed in the following.

NMR Characterization of the Alkali Extracted Lignins

2D HSQC Analysis

^{1}H-^{13}C heteronuclear single quantum coherence spectroscopy (HSQC) analysis revealed the most important structural features of the isolated lignins after the scH_2O treatment. The lignin samples were labelled S1–4 by increasing severity (Table S1). For comparison, spectra of two samples obtained at the lowest and highest severity (S1 and S4, respectively) are reported in Figure 3.

The HSQC spectra of the analysed lignins show the presence of typical hardwood lignin moieties. It is worth of note a very high number of β-O-4 units detected in samples S1–3 in the range 52.3–44.9/100 Ar. This result was further confirmed by quantitative ^{13}C analysis (β-O-4 moieties: 57–42/100 Ar), proving a good correlation between 2D and ^{13}C data as we recently reported.[12,13] The amounts of β-O-4 bonds decreased by 44% from 52.3 to 29.5/100 Ar at severities of 0.28 and 1.66, respectively, (Table 1, entry 4). Noteworthy, the low decrease in β−O–aryl units with increased severity (44%) is in contrast with the results from other biorefinery processes, where they usually decrease by 3–10 times.[47] Similar results were found in our recently reported work on the extraction of lignin from agro-food waste, where a high number of β−O–aryl units was found in the extracted lignins.[14]

The syringyl-to-guiacyl ratio (S/G) kept constant at 2.1 for samples S1–3 and then dropped to 1.8 for S4. This is consistent with a preferred branching and crosslinking for S-units at increased severity as we recently found.[12,13] A slight decrease from 7.7/100 Ar to 6.2/100 Ar in the benzyl ether moieties has

Table 1. Quantification of lignin moieties by 2D HSQC NMR analysis. The results are expressed per 100 Ar.

Entry	Moiety	Integration range δ_C/δ_H (ppm)	Sample			
			S1	S2	S3	S4
1	S/G ratio		2.1	2.1	2.1	1.8
2	Ac	23.1–17.0/2.4–1.5	1.4	1.1	1.2	3.3
3	Cinnamyl alcohol	62.5–59.6/4.2–4.0	2.9	2.9	2.8	2.3
4	**β-O-4/α-OH**	**73.7–69.7/5.3–4.6**	**52.3**	**48.8**	**44.9**	**29.5**
5	Benzyl ether (BE)	83.7–77.9/4.9–4.3	7.7	7.5	7.2	6.2
6	Resinol	86.7–84.1/4.71–4.52	10.1	9.2	9.5	8.2
7	Phenylcoumaran	89.4–85.4/5.72–5.29	2.2	2.3	2.4	1.9
8	GlcU Esters	101.5–100.0/4.72–4.59	0.5	0.3	0.1	0.05
9	PhGly	104.7–99.5/5.23–4.80	0.2	0.2	0.2	0.2
10	Term carbs	94.5–90.0/5.1–4.8 98.6–95.4/5.3–5.0 99.1–94.7/4.5–4.15	0.9	0.6	0.3	0.1
11	Internal carbs	98.6–95.8/4.9–4.5 105.4–98.9/5.3–3.8 107.7–103.7/5.4–5.2	25.6	10.8	6.4	3.5
12	Total carbs[a]		26.5	11.4	6.7	3.6
13	Carb. DP[b]		31	19	22	35
14	Conj S	107.8–104.5/7.5–6.9	15.4	16.0	15.6	13.8
15	Conj COOH	124.1–121.0/7.6–7.4	0.7	0.9	0.8	1.2
16	Vanillyn	126.8–124.4/7.5–7.3	0.6	0.6	0.5	1.0
17	Vinyl–Ar	133.4–126.0/7.4–6.8	5.2	5.0	5.2	7.8
18	Vinyl–Alk	135.5–123.0/6.5–5.8	11.1	11.8	13.3	18.8
19	Ar–CHO	196.8–185.4/10.1–9.3	3.3	2.7	2.4	1.9
20	Fur–CHO	204.2–199.5/9.8–9.5	0.2	0.2	0.2	0.2

[a] Internal + terminal carbohydrates. [b] Average carbohydrates chain length calculated as the ratio between total and terminal carbohydrates.[13]

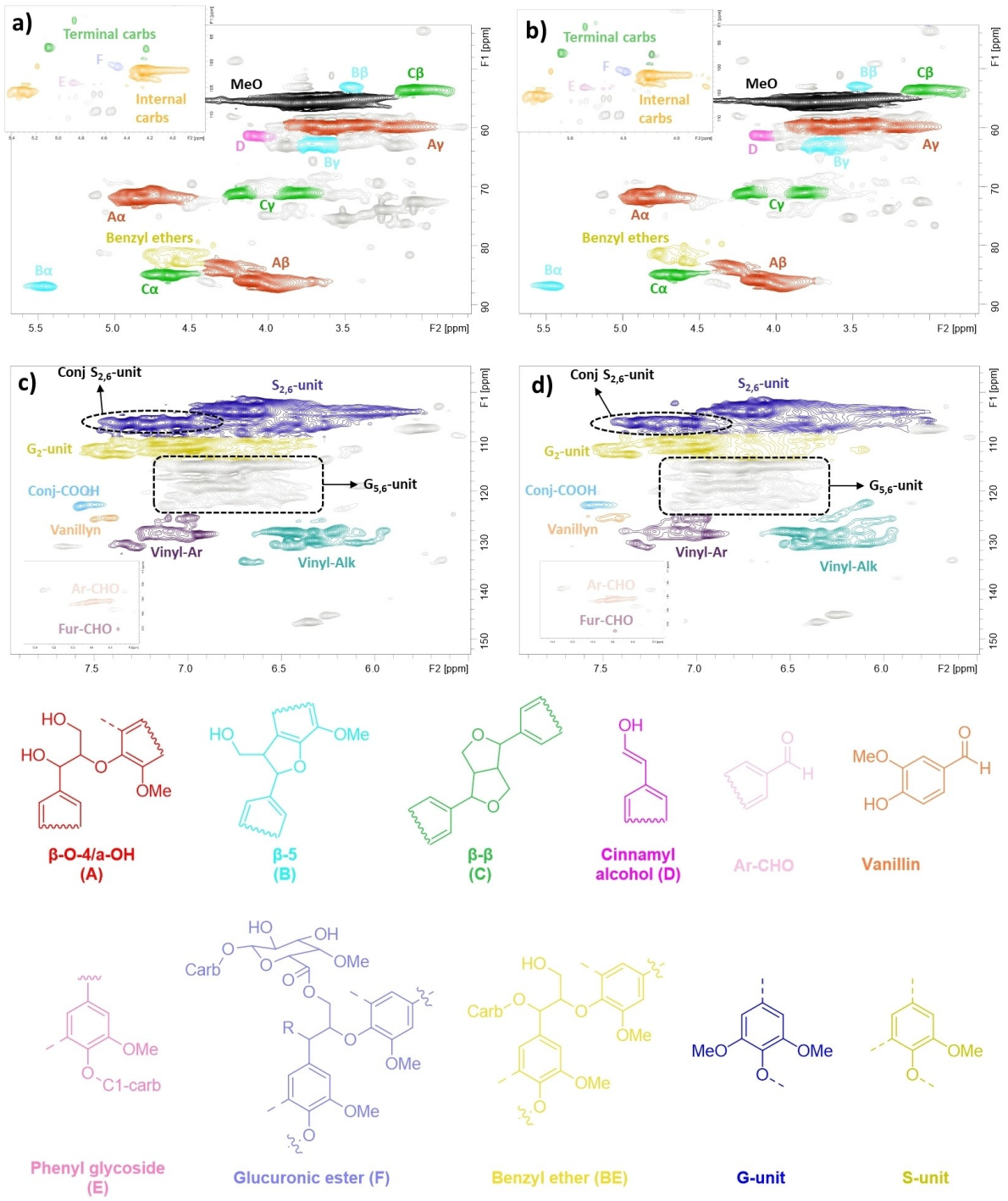

Figure 3. 2D HSQC NMR spectra of lignin samples obtained at low severity (S1; a, c) and high severity (S4; b, d). Only the moieties used for quantification have been highlighted.

been detected between S1 and S4, suggesting that at higher severity water could hydrolyze such bonds (entry 5).

Vinyl–aryl (Vinyl–Ar) and vinyl–alkyl (Vinyl–Alk) chemical bonds were found in large amounts (in the ranges 5.0–7.8/100 Ar and 11.1–18.8, respectively) in all the analyzed samples at $\delta_C/\delta_{H=}$133.4–126.0/7.4–6.8 and 135.5–123.0/6.5–5.8, respectively (entries 17–18).[12] In contrast with our recent results,[12,13] these moieties increased with increased severity. Hence, we found a 33% and 41% increase in the vinyl–aryl and vinyl–alkyl moieties between S1 and S4, respectively. The formation of such bonds could be promoted by the harsh conditions of the scH_2O treatment *via* dehydration of benzyl-type −OH groups (Scheme 1).

The HSQC spectra show a significant presence of lignin carbohydrate linkages, such as phenyl glycoside and γ-ester (Structure E and F in Figure 3) at δ_C/δ_H 99.4–103.7/4.8–5.1 and

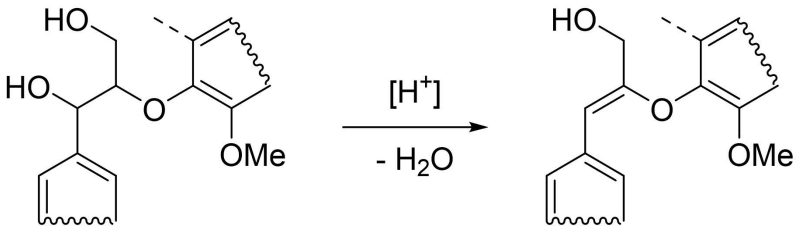

Scheme 1. Possible pathway for the formation of vinyl–aryl units. Here the case of β-O-4 bonds is considered. The acidity is given by the AcOH released via the hydrolysis of acetyl groups in the hemicellulose fraction.[13]

60.8–62.9/4.2–4.4, respectively.[13,53] Benzyl ether (BE) lignin-carbohydrate linkages could be present at δ_C/δ_H 79.6–82.8/4.4–4.9, but they cannot be unequivocally assigned due to the possible overlap of other lignin-lignin benzyl ether signals in the same region.[49] The samples obtained at low severity (S1–2) showed the highest number of lignin carbohydrate complexes (LCCs) in the range 11.4–26.5/100 Ar, while an increase of the severity led to a lower number of LCCs. This could be related to significant hydrolysis of polysaccharides bonds at high severity,[37] as discussed in the previous section. Intriguingly, the average carbohydrates chain length (DP; entry 13), calculated as the ratio between the total and terminal carbohydrates,[13] is quite high in all the analyzed samples in the range 19–35. The average long chain of carbohydrates in LCCs may be an interesting feature for certain applications such as the production of lignin nanoparticles.[13]

The number of β–5 and β–β structures was only slightly affected during the scH_2O treatment (entries 6–7). Clear peaks at δ_C/δ_H = 62.5–59.6/4.2–4.0 and 126.8–124.4/7.5–7.3 suggest the presence of cinnamyl alcohol and vanillin moieties, respectively.[49] In addition, aldehydes of Ar–CHO and Fur–CHO types were detected as well (entries 19–20).

Quantitative ^{13}C NMR Analysis

^{13}C NMR experiments provide reliable quantitative information on different lignin moieties, even if in some cases overlap of signals should be taken into consideration and carefully evaluated case by case.[54,55] β-O-4 bonds are the most abundant linkages in lignin. Milled wood lignin (MWL) is considered to reflect the structure of native lignin, at least at a certain extent.[52] Among arylglycerol–β–aryl structures, the most abundant is the β-O-4/α-OH type (structure A; Figure 3) in addition to other minor β-O-4/α-OR (R = alkyl or aryl) units.[52,55]

^{13}C experiments also provide reliable data on syringyl-to-guaiacyl ratio (S/G), methoxy groups content, and on the degree of condensation (DC) of lignin.[55] Table 2 summarizes the results while the ^{13}C NMR spectra are reported in Figure 4.

The signal of C_γ in structure A at δ_C = 61.4–58.5 (Figure 4 and Figure 5) was used for the quantification of β-O-4 structures in the ^{13}C spectra,[55] as it showed minor overlap with other moieties in the HSQC spectra (see ESI). ^{13}C experiments confirmed the presence of β-O-4 units in high amount for the samples obtained at low severities (S1–3; Table 2, entry 14), showing good correlation with 2D results as we recently found.[12] A very high number (57.0/100 Ar) was found in S1 – obtained at the lowest severity – close to the value of 60/100 Ar for Birch milled wood lignin (BMWL).[55] Worth of note is that such high number of β-O-4 moieties could be attributed to the partial isolation of unreacted wood particles at low severity. This is consistent with the incomplete solubility of S1 in the conventional $CDCl_3$/pyridine mixture for ^{31}P NMR analysis (*vide infra*). Conversely, as expected, an increase of the severity led to a more degraded lignin with a β-O-4 content of 29.1/100 Ar in S4. The low degradation/hydrolysis of β-O-4 linkages during scH_2O treatment may be related to the very short residence time in the reactor (t = 0.3–0.7 s). This allows for the selective hydrolysis of polysaccharides while preserving the lignin structure thanks to a "lightening rod effect" of cellulose and hemicellulose. In other words, the heat-to-mass transfer is favored towards the major biomass components in terms of mass %. Thus, since lignin constitutes only 22.5% of Birch wood,[13] the majority of energy is spent for the hydrolysis of the carbohydrate fractions more than for the degradation/hydrolysis of lignin interlinkage units. To support this theory, our results are in agreement with our recently reported work on the fast scH_2O hydrolysis of polysaccharides using the same reactor.[37] In the latter work, high yields of C-6 and C-5 sugars (61 and 71% w/w, respectively) were obtained at 0.11 s while the formation of degradation products was limited. Such degradation was low in the lignin fraction as well.

The critical role of carbohydrates to protect lignin from degradation is further confirmed by the observed sharp drop of β-O-4 content between S3 and S4 (42 and 29/100 Ar, respectively). The degree of liquefaction topped at the highest severity towards a complete fractionation of the carbohydrate fractions from lignin (Figure 2). Consistently, at the same highest severity the major component of the insoluble fraction is lignin since it has been extracted in 63 wt% yield with respect to the insoluble fraction (Figure 2 and Table S1). As previously discussed, the main target for the reaction is the major mass component. This implies that at the highest severity H_2O preferably targets lignin, being the major component of the insoluble fraction. On the other hand, these considerations are not valid for the lower tested severities where sugars are the most abundant components of the solid fraction.

Low degree of condensation (DC; entry 13) in the range of 0.8 to 5% was found for all the samples. This is an additional confirmation of the low degradation of lignin isolated during all

Table 2. Quantification of lignin moieties by quantitative ^{13}C NMR analysis. The results are expressed per 100 Ar.

Entry	Moiety	Integration range δ_C (ppm)	Sample				
			S1	S2	S3	S4	BMWL[e]
1	CO non-conjugated	210–200	13	6	8	10	3
2	CO conjugated	200–191	15	10	10	9	9
3	Total CO[a]		28	16	18	19	12
4	−COOR non-conjugated	175–168	17	15	12	15	3
5	−COOR conjugated	168–166	2.5	3.5	2.6	3.1	1
6	Total −COOR[b]		20	18	15	18	4
7	−OMe	58–54	141	145	141	123	164
8	S-unit	108.2–103	61	59	59	53	73
9	G-unit	113.6–108.2	28	28	29	32	24
10	S/G ratio[c]		2.2	2.1	2.0	1.6	2.0
11	Ar–H	122.5–103	208	195	199	190	209
13	**DC (%)[d]**		**0.8**	**3.4**	**3.5**	**5.0**	**15**
14	**β-O-4**	**61.4–58.5**	**57**	**47**	**42**	**29**	**60**
15	Oxygenated Aliphatic	90–58	441	222	202	121	260
16	Saturated Aliphatic	54.3–42.9 35.5–0	171	111	112	159	n.a.

[a] Sum of CO (conj + non-conj). [b] Sum of COOR (conj + non-conj). [c] Ratio between S- and G-units. [d] Calculated according to Ref.[56] [e] Birch milled wood lignin; taken from Ref..[55] n.a. = not available.

experiments in this study. These results are pointing out that the recondensation reactions in the aromatic ring were minimized to a low extent.

The S/G ratio kept almost constant for S1–3 at 2.0–2.2, very close to the literature value of 2.0 for BMWL, and then dropped for S4 to 1.6 (entry 10). Consistently with the literature,[12,13] higher severities have been associated with lower S/G ratio, suggesting that syringyl units possess a higher reactivity towards their cleavage compared to guaiacyl moieties at the beginning of the process.

Though the amount of methoxy (−OMe) groups followed the same trend as the S/G ratio, their amount was somewhat lower (*ca.* 11%) when compared to BMWL (compare entries 7 and 10 in Table 2). The effect of the severity on the number of −COOR (esters) was very subtle, and no clear trends could be depicted from ^{13}C results (entries 4–6). Similar conclusions could be drawn for CO carbonyl groups (ketones and aldehydes) except for S1 in which a higher value of 28 CO/100 Ar was found. However, CO groups were higher in samples S1–4 compared to their number in BMWL, most likely due to oxidation reactions occurring during the scH_2O treatment.

^{31}P NMR Analysis

Phenolic and aliphatic hydroxyls are key functional groups for the use of lignin in high value applications.[57,58] For instance, a high number of phenolic −OH groups is beneficial for an improved performance of lignin as adhesive[59] and as an antioxidant.[40] To date, ^{31}P NMR is among the best techniques to evaluate their amount. Table 3 reports the results for samples S2–4. However, S1 was only partially soluble both in the conventional $CDCl_3$/pyridine solvent system and others (i.e., DMF and ionic liquid based)[51] and, thus, it was not possible to conduct the ^{31}P NMR experiment for this sample (see also experimental).

Aliphatic −OH groups decreased with increased severity from 5.25 mmol/g to 3.37 mmol/g in S2 and S4, respectively.

Table 3. Quantification of -OH and −COOH groups in the lignin samples by ^{31}P NMR.

Entry	Sample	Severity	Functionality (mmol/g)						
			Aliphatic	5-subst.	G-non conj	H-type PhOH	−COOH	Total PhOH	Total –OH
1	S2	0.71	5.25	0.91	0.41	0.09	0.39	1.41	6.66
2	S3	1.18	4.92	1.05	0.47	0.12	0.48	1.63	6.55
3	S4	1.66	3.37	1.51	0.63	0.17	0.73	2.31	5.68
4	BMWL[a]		5.67	0.67	0.51		0.28	1.18	6.85

[a] Birch Milled Wood Lignin taken from Ref..[50]

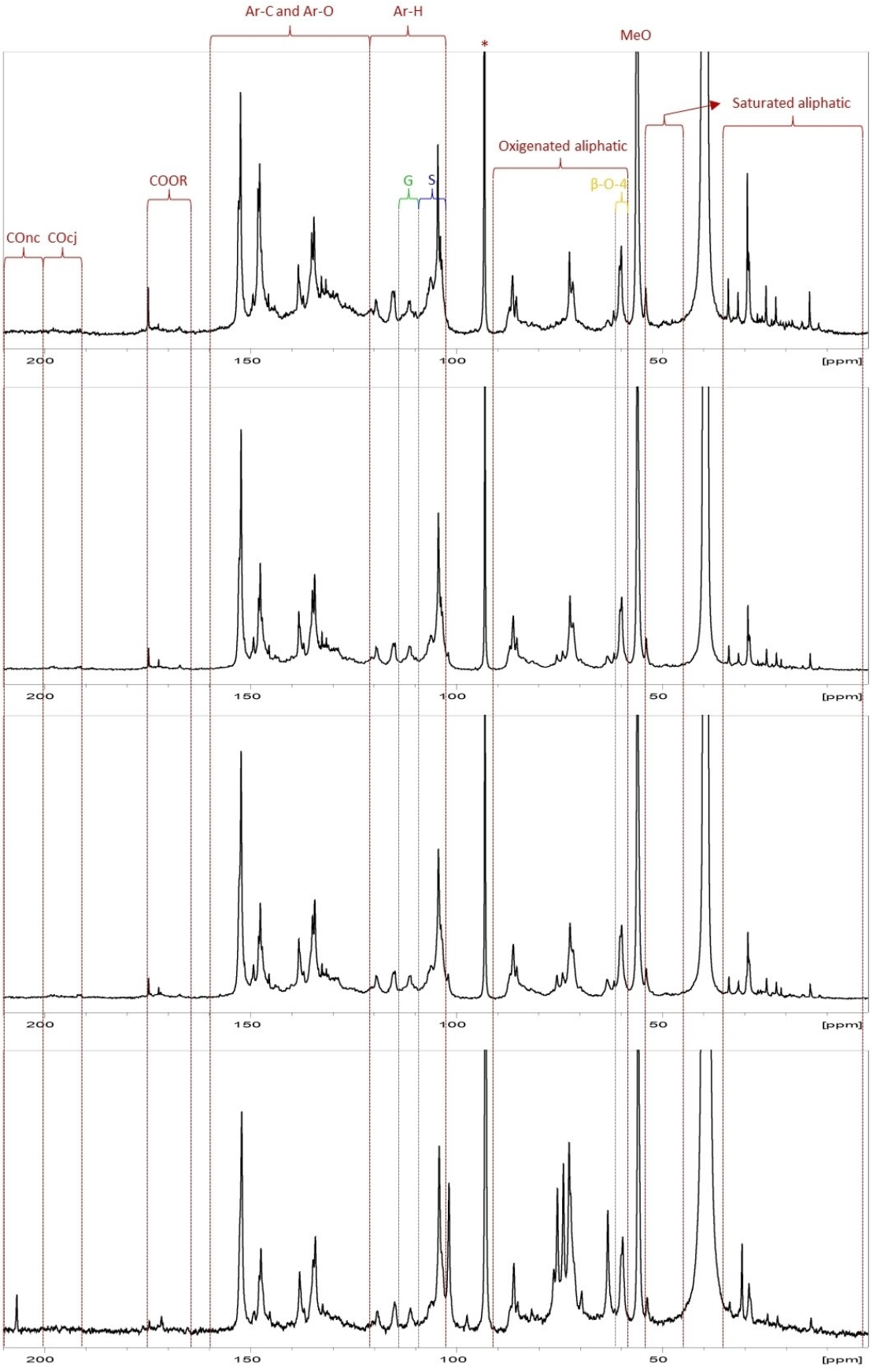

Figure 4. ^{13}C spectra of samples S1–4. The ranges for the integration of different lignin units are evidenced.

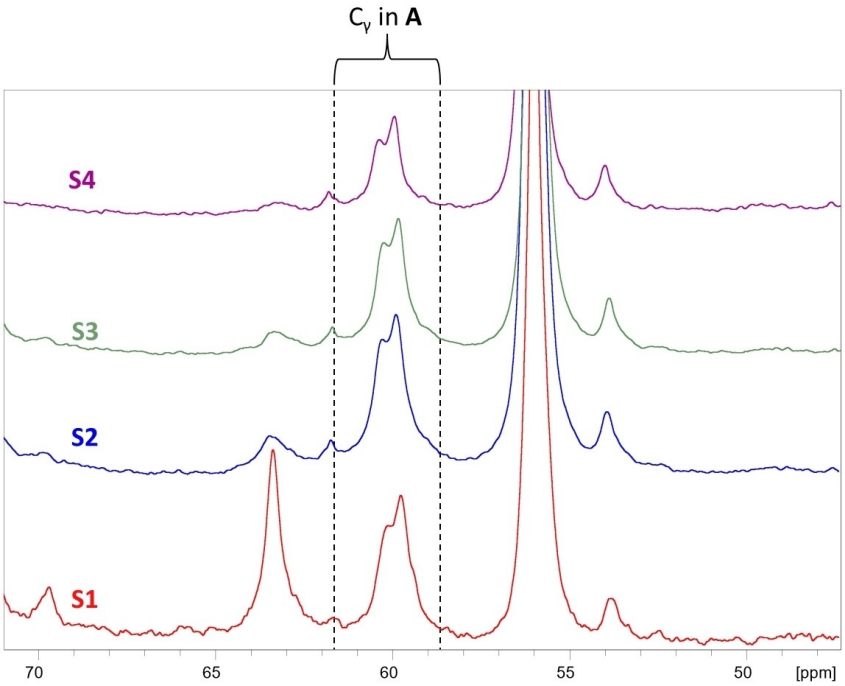

Figure 5. Expanded regions of the ^{13}C spectra of samples S1–4. The signal of C_γ in β-O-4 (structure **A**) moieties is evidenced.

Consequently, the total amount of −OH groups followed a similar deceasing trend from 6.66 mmol/g to 5.68 mmol/g in S2 and S4, respectively. This is consistent with a scH_2O-promoted acid catalyzed dehydration of lignin occurring through aliphatic −OH groups, as depicted in Scheme 1. In addition, a contribution to the number of aliphatic −OHs from carbohydrates present in the samples obtained at low severities should be considered as well.

During the course of the reaction, phenolic −OH increased from 1.41 mmol/g to 2.31 mmol/g in S2 and S4, respectively, consistently with the observed cleavage of β-O-4 bonds at increased severity (Table 2, entry 14). The observed increasing number of 5-substituted phenolic −OH at higher severity is consistent with the slight increase in the DC (Table 2, entry 13). Parallelly, the decrease of S/G ratio with increased severity well correlates with the increase of G-types phenolics (compare Table 2 and Table 3).

An increasing trend from 0.39 mmol/g to 0.73 mmol/g was detected for −COOH groups in S2 and S4, respectively. Since ester groups were almost constant with increased severity (Table 2, entry 6), this suggests that during the scH_2O treatment oxidation of −OH and CO groups occurred. Noteworthy, the occurrence of oxidation reactions was hypothesized based on the ^{13}C NMR results as well (see previous section).

The amount and type of −OH groups in S2 correlates with BMWL (compare entries 1 and 4). This is especially true for aliphatic and total −OH groups, which differ for less than 8% and 3% between S2 and the reference BMWL, respectively. Nevertheless, higher phenolic −OH and −COOH (*ca.* 16% and 28%, respectively) were detected in S2 with respect to BMWL, suggesting that the cleavage of certain types of aryl–O–R bonds occurred during the scH_2O treatment, even if at a low extent. As expected, the correlation became worse for the samples obtained at higher severities (S3–4; compare entries 2–4). All these results also suggest that the correlation between BMWL and S1 (not soluble) may be even higher than the one of S2.

Thermal Properties and Molar Mass Distribution

The glass transition temperature, the molar mass (MM), and the molar mass distribution (MMD) are important properties which impact lignin performance in various applications.[60,61]

MM and MMD have been evaluated by size exclusion chromatography (SEC) using sulfonated polystyrene standards for calibration (see experimental). As SEC relies on the separation of molecules based on their hydrodynamic radius,[62,63] this suggests that the presence of carbohydrates heavily influences the volume and morphology of the lignin samples in solution. In other words, the MM and MMD of the samples with the same (or similar) amount of carbohydrates mainly depends on the molecular weight distribution of lignin, while high carbohydrates content could bring to a misleading estimation of the MMD for a certain sample.

This discussion is consistent with the results reported in Table 4. Hence, the highest molecular weight was found in S1 characterized by the highest carbohydrates content (Table 4, entry 1 and Table 1, entry 12). Then, when comparing samples with similar carbohydrate contents (S2–4, entries 2–4), a clear dependence of the MMD on the severity was noticed. A decrease in both M_n and M_w was observed passing from S2 to S4. This is in line with the cleavage (hydrolysis) of β-O-4 bonds at increased severity with an almost constant DC as previously discussed (Table 2).

Table 4. Molar mass distribution of the lignin samples.

Entry	Sample	M_n (g/mol)	M_w (g/mol)	D
1	S1	3219	14260	4.4
2	S2	2183	9817	4.5
3	S3	2155	7993	3.7
4	S4	1789	5727	3.2

Table 5. Thermal degradation of the lignin samples.

Sample	T_{onset} (°C)	T_{max} (°C)	T_{50} (°C)	Weight-% by the end of measurement
S1	250	347	352	24.63
S2	185	270	308	18.22
S3	151	256	309	25.66
S4	112	245	230	25.48

Generally, high MMD has been associated to high T_g and *vice versa*.[64] Both conventional DSC and modulated DSC (mDSC) measurements were carried out on the lignin samples providing two separate results for the glass transition temperatures (T_g and T_g', respectively). Prior to the evaluation of the glass transition temperature of the samples, thermo-gravimetry analysis was performed to evaluate their thermal stability (Figure 6 and Table 5).

Noteworthy, the DSC curves of samples S3 and S4 did not show a clear T_g. This can be due to weak self-interactions (i.e., H-bonding) of the lignin units which hide the glass transition. Similar difficulties in detecting the T_g of lignin have been previously reported in the literature.[65–67] The highest glass transition temperature (T_g = 133 °C and T_g' = 139 °C) was found in S1. Consistently with its molar mass decrease, a lower T_g was noticed for S2 (T_g = 120 °C and T_g' = 116 °C), obtained at a higher severity.

Overall, the CF scH_2O treatment allowed to tune the properties such as the molar mass and the glass transition temperature of the isolated lignins by simply varying the reaction severity. This avoids tedious modification procedures which are generally requested to modify/tune the lignin properties.[68,69]

Conclusions

We herein demonstrated that the continuous flow scH_2O treatment of Birch wood followed by alkali extraction of lignin from the treated solids is a valuable process to isolate lignin and lignin carbohydrate complexes (LCCs) with a high number of β-O-4 moieties. Depending on the reaction severity, lignin/LCCs with β-O-4 moieties in the range 29–57/100 Ar were isolated in 13–19 wt% yield with respect to the initial wood. To explain such high number of β-O-4 moieties a "lightning rod effect" of polysaccharides has been claimed. Our results suggest that for very short reaction times (0.3–0.7 s) a preferential

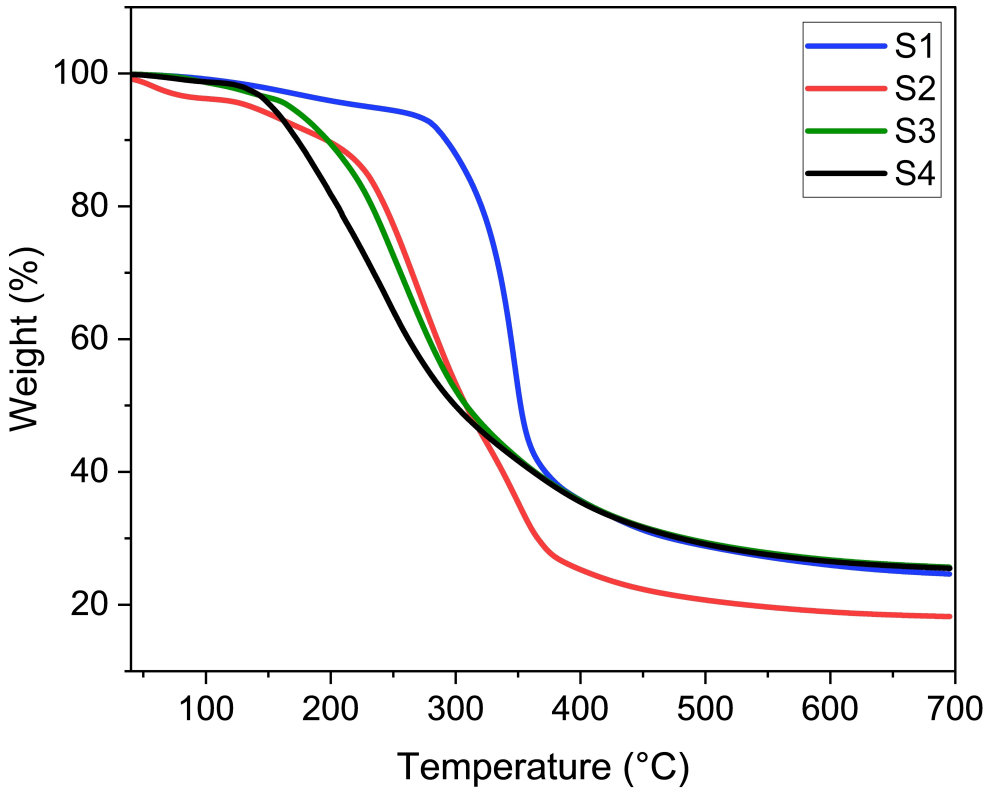

Figure 6. Thermograms of samples S1-4.

hydrolysis of polysaccharide chains occurs in place of lignin degradation.

The comprehensive NMR characterization (HSQC, ^{13}C and ^{31}P) provided further insights on the structure of the isolated lignins. A low degree of condensation (DC) < 5% was found for all the lignin samples. The structure and properties of the samples obtained at low severity were close to Birch milled wood lignin. The results obtained from different NMR experiments well correlated each other, providing reliable support to the discussed outcomes. To conclude, a dependence of the glass transition temperature and the molar mass distribution on the reaction severity was found. Higher severity led to lower T_g and a decreased molecular weight of the lignin samples. This process represents a simply and green way to modify the properties of lignin without the need for any chemical modification.

Overall, in our vision, such an approach may be extended to other biomass feedstocks, enabling for the isolation of non-degraded lignins/LCCs with tunable structure and properties.

Author Contributions

D.R.: Investigation, methodology, conceptualization, supervision, writing-reviewing and editing; T.A.: Investigation, methodology, writing. E.C.: Methodology, reviewing; D.D.: Investigation, methodology; M.A.: Investigation, methodology, writing. D.T.: Investigation, methodology, writing; C.X.: supervision and funding acquisition; D.C.: Conceptualization, supervision, writing, and funding acquisition; M.B.: Conceptualization, supervision, and funding acquisition.

Acknowledgments

This work is dedicated to Prof. of practice Dr. Mikhail Balakshin. Prof. Chunlin Xu is thankfully acknowledged for his help in the data discussion. The authors acknowledge the Agencia Estatal de Investigación for the financial support given in Project PID2020–119249RA–I00. This work was supported by the Regional Government of Castilla y León (Spain) and the EU-FEDER program (CLU-2019-04). D.C. is funded by the Spanish Ministry of Science, Innovation and Universities ("Beatriz Galindo" fellowship BEAGAL18/00247). D.R., D.D. and M.B gratefully acknowledge the support from the Research Council of Finland (former Academy of Finland, grant decision number 341586). In addition, this work was a part of the Academy of Finland's Flagship Programme under Projects No. 318890 and 318891 (Competence Center for Materials Bioeconomy, FinnCERES).

Conflict of Interests

There are no conflicts of interest to declare.

Data Availability Statement

The data that support the findings of this study are available in the supplementary material of this article.

Keywords: Lignin · Lignin carbohydrate complexes (LCCs) · NMR · Supercritical water · DSC · GPC

[1] M. Brienzo, S. Ferreira, M. P. Vicentim, W. de Souza, C. Sant'Anna, *Bioenergy Res.* **2014**, *7*, 1454–1465.
[2] A. Lorenci Woiciechowski, C. J. Dalmas Neto, L. Porto de Souza Vandenberghe, D. P. de Carvalho Neto, A. C. Novak Sydney, L. A. J. Letti, S. G. Karp, L. A. Zevallos Torres, C. R. Soccol, *Bioresour. Technol.* **2020**, *304*, 122848–122857.
[3] M. Foston, A. J. Ragauskas, *Ind. Biotechnol.* **2012**, *8*, 191–208.
[4] A. Lorenci Woiciechowski, C. J. Dalmas Neto, L. Porto de Souza Vandenberghe, D. P. de Carvalho Neto, A. C. Novak Sydney, L. A. J. Letti, S. G. Karp, L. A. Zevallos Torres, C. R. Soccol, *Bioresour. Technol.* **2020**, *304*, 122848.
[5] V. Oriez, J. Peydecastaing, P. Y. Pontalier, *Molecules* **2019**, *24*, 4273.
[6] A. T. Hoang, S. Nizetic, H. C. Ong, C. T. Chong, A. E. Atabani, V. V. Pham, *J. Environ. Manage.* **2021**, *296*, 113194.
[7] C. Álvarez, F. M. Reyes-Sosa, B. Díez, *Microb. Biotechnol.* **2016**, *9*, 149–156.
[8] S. Sun, S. Sun, X. Cao, R. Sun, *Bioresour. Technol.* **2016**, *199*, 49–58.
[9] Y. H. Jung, K. H. Kim, Acidic Pretreatment, in: *Pretreatment of Biomass – Processes and Technologies*, **2015**, pp. 27–50. Copyright 2015 Elsevier B.V. https://doi.org/10.1016/B978-0-12-800080-9.00003-7
[10] G. Garrote, H. Domínguez, J. C. Parajó, *Holz Roh Werkst.* **1999**, *57*, 191–202.
[11] H. Sarip, M. S. Hossain, M. N. Mohamad Azemi, K. Allaf, *BioResources* **2016**, *11*, 10625–10653.
[12] P. Schlee, D. Tarasov, D. Rigo, M. Balakshin, *ChemSusChem* **2023**, *16*, e202300549.
[13] D. Tarasov, P. Schlee, A. Pranovich, A. Moreno, L. Wang, D. Rigo, M. H. Sipponen, C. Xu, M. Balakshin, *Green Chem.* **2022**, *24*, 6639–6656.
[14] T. Adamovic, D. Tarasov, E. Demirkaya, M. Balakshin, M. J. Cocero, *J. Cleaner Prod.* **2021**, *323*, 129110.
[15] D. A. Cantero, C. Martínez, M. D. Bermejo, M. J. Cocero, *Green Chem.* **2015**, *17*, 610–618.
[16] D. A. Cantero, L. Vaquerizo, C. Martinez, M. D. Bermejo, M. J. Cocero, *Catal. Today* **2015**, *255*, 80–86.
[17] A. Romero, D. A. Cantero, A. Nieto-Márquez, C. Martínez, E. Alonso, M. J. Cocero, *Green Chem.* **2016**, *18*, 4051–4062.
[18] K. Ehara, S. Saka, H. Kawamoto, *J Wood Sci.* **2002**, *48*, 320–325.
[19] N. Akiya, P. E. Savage, *Chem. Rev.* **2002**, *102*, 2725–2750.
[20] K. Ehara, D. Takada, S. Saka, *J. Wood Sci.* **2005**, *51*, 256–261.
[21] K. Yoshida, J. Kusaki, K. Ehara, S. Saka, *Appl. Biochem. Biotechnol.* **2005**, *123*, 795–806.
[22] M. Osada, T. Sato, M. Watanabe, M. Shirai, K. Arai, *Combust. Sci. Technol.* **2006**, *178*, 537–552.
[23] A. C. P. Borges, J. A. Onwudili, H. M. C. Andrade, C. T. Alves, A. Ingram, S. A. B. Vieira de Melo, E. A. Torres, *Fuel* **2019**, *255*, 115804.
[24] T. L. K. Yong, Y. Matsumura, *Ind. Eng. Chem. Res.* **2012**, *51*, 5685–5690.
[25] J. A. Onwudili, P. T. Williams, *RSC Adv.* **2013**, *3*, 12432–12442.
[26] J. A. Okolie, R. Rana, S. Nanda, A. K. Dalai, J. A. Kozinski, *Sustainable Energy Fuels* **2019**, *3*, 578–598.
[27] J. M. L. Penninger, M. Rep, *Int. J. Hydrogen Energy* **2006**, *31*, 1597–1606.
[28] P. Azadi, R. Farnood, *Int. J. Hydrogen Energy* **2011**, *36*, 9529–9541.
[29] S. N. Reddy, S. Nanda, A. K. Dalai, J. A. Kozinski, *Int. J. Hydrogen Energy* **2014**, *39*, 6912–6926.
[30] M. J. Cocero, Á. Cabeza, N. Abad, T. Adamovic, L. Vaquerizo, C. M. Martínez, M. V. Pazo-Cepeda, *J. Supercrit. Fluids* **2018**, *133*, 550–565.
[31] Y. Qian, C. Zuo, J. Tan, J. He, *Energy* **2007**, *32*, 196–202.
[32] P. Azadi, S. Khan, F. Strobel, F. Azadi, R. Farnood, *Appl. Cat., B* **2012**, *117–118*, 330–338.
[33] F. Gomollón-Bel, J. García-Martínez, *Angew. Chem. Int. Ed.* **2023**, *62*, e202218975.
[34] E. Drioli, A. Brunetti, G. Di Profio, G. Barbieri, *Green Chem.* **2012**, *14*, 1561–1572.
[35] B. Gutmann, D. Cantillo, C. O. Kappe, *Angew. Chem. Int. Ed.* **2015**, *54*, 6688–6728.

[36] F. Mattea, Á. Martín, M. J. Cocero, *J. Food Eng.* **2009**, *93*, 255–265.
[37] C. M. Martínez, T. Adamovic, D. A. Cantero, M. J. Cocero, *J. Supercrit. Fluids* **2019**, *143*, 242–250.
[38] D. A. Cantero, A. Álvarez, M. D. Bermejo, M. J. Cocero, *J. Supercrit. Fluids* **2015**, *98*, 204–210.
[39] M. M. Abu-Omar, K. Barta, G. T. Beckham, J. S. Luterbacher, J. Ralph, R. Rinaldi, Y. Román-Leshkov, J. S. M. Samec, B. F. Sels, F. Wang, *Energy Environ. Sci.* **2021**, *14*, 262–292.
[40] D. Diment, O. Tkachenko, P. Schlee, N. Kohlhuber, A. Potthast, T. Budnyak, D. Rigo, M. Balakshin, *Biomacromolecules* **2023**, *25*, 1–4.
[41] M. Galkin, *Curr. Opin. Green Sustainable Chem.* **2021**, *28*, 100438.
[42] M. Talebi Amiri, G. R. Dick, Y. M. Questell-Santiago, J. S. Luterbacher, *Nat. Protocol.* **2019**, *14*, 921–954.
[43] H. Zhou, J. Y. Xu, Y. Fu, H. Zhang, Z. Yuan, M. Qin, Z. Wang, *Green Chem.* **2019**, *21*, 4625–4632.
[44] A. Rahimi, A. Ulbrich, J. J. Coon, S. S. Stahl, *Nature* **2014**, *515*, 249–252.
[45] M. Karlsson, V. L. Vegunta, R. Deshpande, M. Lawoko, *Green Chem* **2022**, *24*, 1211–1223.
[46] J. S. Rodrigues, A. D. S. M. de Freitas, C. C. Maciel, C. Guizani, D. Rigo, M. Ferreira, M. Hummel, M. Balakshin, V. R. Botaro, *Int. J. Biol. Macromol.* **2023**, *240*, 124460.
[47] E. A. Capanema, M. Y. Balakshin, J. F. Kadla, *J. Agric. Food. Chem.* **2004**, *52*, 1850–1860.
[48] M. Balakshin, E. Capanema, *J. Wood Chem. Technol.* **2015**, *35*, 220–237.
[49] M. Y. Balakshin, E. A. Capanema, X. Zhu, I. Sulaeva, A. Potthast, T. Rosenau, O. J. Rojas, *Green Chem.* **2020**, *22*, 3985–4001.
[50] M. Balakshin, E. Capanema, *J. Wood Chem. Technol.* **2015**, *35*, 220–237.
[51] I. Sumerskii, P. Korntner, G. Zinovyev, T. Rosenau, A. Potthast, *RSC Adv.* **2015**, *5*, 92732–92742.
[52] E. A. Capanema, M. Y. Balakshin, J. F. Kadla, *J. Agric. Food. Chem.* **2005**, *53*, 9639–9649.
[53] M. Y. Balakshin, E. A. Capanema, H. M. Chang, *Holzforschung* **2007**, *61*, 1–7.
[54] M. Y. Balakshin, E. A. Capanema, *RSC Adv.* **2015**, *5*, 87187–87199.
[55] M. Y. Balakshin, E. A. Capanema, R. B. Santos, H. M. Chang, H. Jameel, *Holzforschung* **2016**, *70*, 95–108.
[56] M. Y. Balakshin, E. A. Capanema, R. B. Santos, H. M. Chang, H. Jameel, *Holzforschung* **2016**, *70*, 95–108.
[57] X. Jiang, J. Liu, X. Du, Z. Hu, H. M. Chang, H. Jameel, *ACS Sustainable Chem. Eng.* **2018**, *6*, 5504–5512.
[58] D. Di Francesco, D. Rigo, K. Reddy Baddigam, A. P. Mathew, N. Hedin, M. Selva, J. S. M. Samec, *ChemSusChem* **2022**, *15*, e202200326.
[59] M. Zhao, J. Jing, Y. Zhu, X. Yang, X. Wang, Z. Wang, *Int. J. Adhes. Adhes.* **2016**, *64*, 163–167.
[60] C. Wang, S. S. Kelley, R. A. Venditti, *ChemSusChem* **2016**, *9*, 770–783.
[61] M. Y. Balakshin, E. A. Capanema, I. Sulaeva, P. Schlee, Z. Huang, M. Feng, M. Borghei, O. J. Rojas, A. Potthast, T. Rosenau, *ChemSusChem* **2021**, *14*, 1016–1036.
[62] O. Musl, S. Galler, G. Wurzer, M. Bacher, I. Sulaeva, I. Sumerskii, A. K. Mahler, T. Rosenaus, A. Potthast, *Biomacromolecules* **2022**, *23*, 1413–1422.
[63] S. Podzimek, *Light Scattering, Size Exclusion Chromatography and Asymmetric Flow Field Flow Fractionation: Powerful Tools for the Characterization of Polymers, Proteins and Nanoparticles*, Wiley **2010**, 1, ISBN: 978-1-118-10272-5.
[64] A. L. Agapov, A. P. Sokolov, *Macromolecules* **2009**, *42*, 2877–2878.
[65] J. Lisperguer, P. Perez, S. Urizar, *J. Chil. Chem. Soc.* **2009**, *54*, 460–463.
[66] G. M. Irvine, *Wood Sci. Technol.* **1985**, *19*, 139–149.
[67] W. G. Glasser, R. K. Jain, *Holzforschung* **1993**, *47*, 225–233.
[68] P. Figueiredo, K. Lintinen, J. T. Hirvonen, M. A. Kostiainen, H. A. Santos, *Prog. Mater Sci.* **2018**, *93*, 233–269.
[69] E. A. Agustiany, M. Rasyidur Ridho, *Polym. Compos.* **2022**, *43*, 4848–4865.

Manuscript received: July 30, 2024
Revised manuscript received: September 23, 2024
Accepted manuscript online: September 24, 2024
Version of record online: November 6, 2024